"Research Note"

THE EFFECT OF NON-UNIFORM AIR-GAP ON THE NOISE IN SWITCHED RELUCTANCE MOTORS[*]

A. DADPOUR[**] AND K. ANSARI

Dept. of Electrical Engineering, Faculty of Engineering, Ferdowsi University of Mashhad, Mashhad, I. R. of Iran
Email: a.dadpour@gu.ac.ir

Abstract– The major problems in switched reluctance motors (SRMs) are radial force and torque ripple which cause increased undesirable acoustic noise. This paper describes an approach to determine optimum magnetic circuit parameters to minimize both radial force and torque ripple for such motors. There is no publication for simultaneous reduction of both radial force and torque ripple. In previous works, torque ripple was decreased without any research on the radial force or counter. In this paper, a procedure for radial force and torque ripple reduction in SR motors is proposed. To decrease the acoustic noise, the air gap width is increased while the radial force is maximized. On the other hand, by increasing the air gap width, torque decreases. By varying the angular interval and consequently the air gap width, the optimum angular interval is achieved. In the optimum angular interval, the radial force decreases while the torque remains constant. A two-dimensional (2-D) finite element (FE) analysis carried out on the 6/4 SRM. By using the method of the compensated current, the ripple torque can be reduced to zero, radial force decreases 3.7%, and the acoustic noise power decreases 7.3% in the non-uniform air gap in comparison with the static case. Radial force decreases 5.6% and the acoustic noise power decreases 10.9% in the uniform air gap in comparison with the static case.

Keywords– Switched reluctance motor, radial force, torque ripple, acoustic noise

1. INTRODUCTION

Recently, the switched reluctance motor (SRM) was studied for high-speed application because of its simple structure and development of power electronics. SRMs develop torque through an interaction between the electromagnetic excitation from the stator poles and the rotor teeth. Once a particular combination of phase currents is established and maintained in the stator, the rotor teeth will be attracted into alignment with the stator poles in a particular position. This attraction force can be divided into tangential and radial force components relative to the rotor. The tangential force is converted into the rotational torque. It contains a significant radial force component in addition to the required tangential force [1].

The dominant source of the acoustic noise in the SRM has been shown to be the distortion of the stator by radial magnetic force. The other problem for SRMs is torque ripple which causes increased undesirable acoustic noise. It is also caused by the saliency of the stator and rotor [2].

Acoustic noise reduction in SRM drive shows that some researchers worked on operating parameters of a switched reluctance drive. They changed some parameters such as the magnitude of phase currents and the time that these currents turned on or off. As a result of these changes, torque ripple was minimized [3, 4]. Some researchers minimized the radial force by changing these parameters [5]. In several papers, the shapes of rotor and stator poles were studied to decrease the torque ripple [6-10] or magnetic radial force [11].

All of the mentioned studies have been done separately on either the torque ripple or radial magnetic force reduction. On the other hand, in these works torque ripple was decreased without any research on the radial force or counter. However, when torque ripple is decreased the radial force may be increased or decreased.

In this paper, the geometry of low magnetic radial force together with torque ripple was studied and a motor having arcuate teeth was proposed. Its characteristics are simulated by finite element method (FEM) analysis and compared with SRMs having conventional shape. Optimum arcs of the stator and rotor pole of an SRM have been obtained by carrying out extensive two-dimensional (FE) analysis for a motor having the well-known 6/4 configurations.

2. MAGNETIC SOURCES OF NOISE

Radial force and torque ripple are the dominant sources of the acoustic noise in SRM. Each of these sources is carried out in this section.

a) Radial force

The magnetic flux in the SRM passes across the air gap in an approximate radial direction producing radial, tangential, and lateral forces on the stator and rotor. To determine the relationship between these forces and the SRM dimensions, the SRM is assumed to be operating in the linear region. Figure 1 illustrates the various dimensions involved in the derivation of these forces.
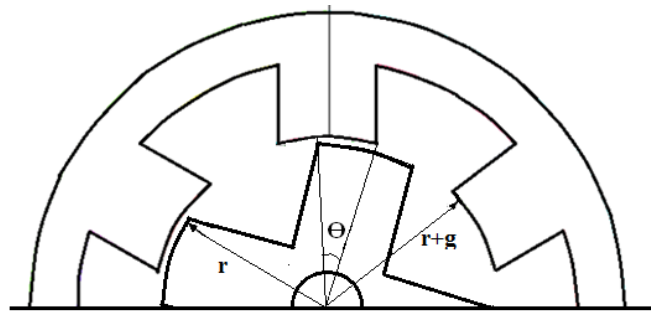

Fig. 1. Various dimensions of SRM

Consider that iron is infinitely permeable and has zero reluctance which leaves only the air gap to provide reluctance in the circuit. The air gap flux density at a given stator and rotor pole overlap angle (θ), air gap (l_g), and current (i) is given as $B_g(\theta,i,l_g)$. Let r be the outer radius of the rotor, l be the stack length or iron length in the z direction, T_{ph} be the number of turns in one phase of the machine, H_g be the magnetic field strength, ϕ be the flux, and μ_0 be the permeability of air. Then the flux linkage is derived as:

$$\psi(\theta,i) = T_{ph}\phi = T_{ph}B_g A = T_{ph}\mu_0 H_g lr\theta$$

$$\psi(\theta,i) = T_{ph}\mu_0\frac{T_{ph}i}{l_g}lr\theta = \mu_0\frac{T_{ph}^2}{l_g}lr\theta i \tag{1}$$

The co-energy is given by:

$$W'(\theta,i) = \int \psi(\theta,i)di = \int \mu_0\frac{T_{ph}^2}{l_g}lr\theta i.di$$

$$W'(\theta,i) = \mu_0\frac{T_{ph}^2}{2l_g}lr\theta i^2 \tag{2}$$

It can be seen that the co-energy, $W'(\theta,i)$ is a state function of the four independent variables θ, i, l_g, and l. Thus, its differential (radial force, lateral force and electromagnetic torque) can be expressed as:

$$F_r = -\frac{\partial W'(\theta,i,l_g)}{\partial l_g} = \frac{\mu_0 l r \theta T_{ph}^2}{2 l_g^2} i^2 \qquad (3)$$

$$T = \frac{\partial W'(\theta,i)}{\partial \theta} = \frac{\mu_0 r l T_{ph}^2}{2 l_g} i^2 \qquad (4)$$

The Eqs. (3) and (4) show that radial force is usually multiple times that of the tangential force in the SRM. Such a large force causes stator vibrations. Moreover, the Eqs. (3) and (4) show that radial force and torque are dependent on design parameters and square of phase current. Some of these parameters are common in two equations, and some like θ and l_g are able to produce different effects on radial force and torque.

In addition to these parameters, the leakage flux, iron circuit reluctance, and saturation effect on radial force and torque are also involved. It is difficult to obtain the relation between these all phenomena and the radial force and torque. So the machine should be simulated to see the effect of all these on the radial force and/or torque.

b) Acoustic noise intensity

The magnitude of the acoustic noise at any operating condition depends on the extent of circumferential deflection due to the radial force wave (in N/m), which is the radial force per unit operating area. Sound power radiated by an electric machine can be expressed as [12]:

$$P = 4\sigma_{rel}.\rho.c.\pi^2.f_{exc}^2.D_{circum}^2.R_{out}.l \qquad (5)$$

where c is the traveling speed of sound (m/s) in the medium, ρ is the density of air, R_{out} is the outer radius of the stator (m), l is the stack length or iron length in the z direction, f_{exc} is the excitation frequencies (Hz) and σ_{rel} is the relative sound intensity and equal to:

$$\sigma_{rel} = \frac{k^2}{1+k^2}$$

where k is the wave number and equal to:

$$k = \frac{2\pi.R_{out}.f_{exc}}{c}$$

Amplitude of dynamic deflection is equal to:

$$D_{cicum}(f_{exc}) = \frac{\dfrac{12 F_{r_{per}}(f_{exc}) R_c}{m^4 E}(\dfrac{R_c}{h_s})^3}{\sqrt{(1-(\dfrac{f_{exc}}{f_m})^2)^2 + (\dfrac{\delta}{\pi}\dfrac{f_{exc}}{f_m})^2}} \qquad (6)$$

where $F_{r_{per}}$ is the Amplitude of radial force wave (N/m). R_c and h_s are the mean radius of stator yoke and the stator pole height, respectively. m and f_m are circumferential mode number and mode frequency, respectively. E is the modulus of elasticity of stator material. δ is the logarithmic decrement and is equal to $\delta = 2\pi\varsigma$, where ς is the damping ratio and equal to:

$$\varsigma = \frac{c}{\sqrt{4kM}}$$

k and *M* are the equivalent stiffness and mass, respectively. Excitation frequencies equal to:

$$f_{exc}(n) = n f_p = \frac{n \omega_m N_{rp}}{60} \qquad (7)$$

where N_{rp}, ω_m and f_p are the number of rotor poles, the rotation speed of the machine (r/min), and the fundamental frequency of phase current (Hz),respectively.

The equations (5) and (6) show that the radiated sound power is proportional to the squared amplitude of the radial force. Therefore, to decrease the radiated sound power, we must find a way to decrease the radial force.

c) Torque ripple

If the SR motor is running and the torque value is not constant, we have torque ripples and acoustic noise. The expression for the torque ripple is [7]:

$$Torque\ Ripple = \frac{T_{max} - T_{min}}{T_{av}} \qquad (8)$$

To reduce noise, the torque ripple must be decreased. The average torque is found over the portion of the torque profile, which is actually utilized in the motor. In a 6/4 SRM, one phase will be excited for 30° only. For the commutation purpose, the excitation will be slightly more. The next phase will be switched on after 30° rotation of the motor. Therefore, taking an average over the 30° is recommended. The authors would like to select that 30° where the torque is nearly constant. This choice will ensure maximum average torque with minimum ripple.

3. SRM SIMULATION BY USING FE METHOD

Table 1 shows dimensions of the used three-phase 6/4 SR motor. Both the permeability of the air and the winding are 1. The materials of the stator laminating and the rotor laminating are considered equal to 0.5mm by using BH magnetizing curve which has been shown in Fig. 2. Finite element analysis software, ANSYS, has been used to build and solve nonlinear magnetic 2-D model of the SRM.

Table 1. Dimensions and material data of the original motor

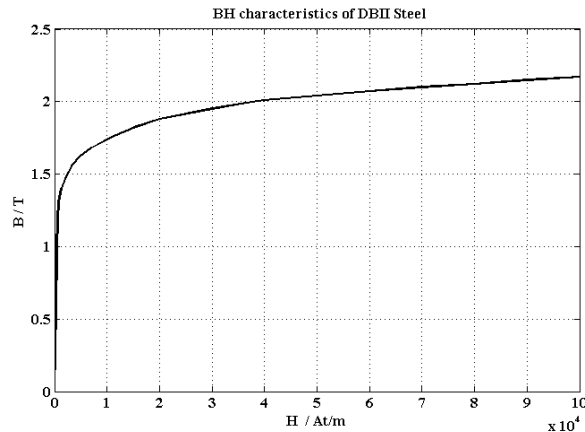|	
Number of stator poles	6
Number of rotor poles	4
Stator outer diameter	12.4 cm
Air gap length	0.04 cm
Stator inner diameter	7.16 cm
Number of turns/phase	180
Stator pole height	1.62 cm
Stator pole arc	40 degree
Stator back iron thickness	1 cm
Rotor pole arc	42 degree
Rotor outer diameter	7.12 cm
Rotor pole height	2.1 cm
Stator and rotor core material	DBII steel
Stack depth	3.74 cm

Fig. 2. BH magnetizing curve of stator and rotor laminating

Simulating results show that, increasing the current increases the flux density, the torque and radial force are maximized at the same rotor angle, and increase when the phase current increases, the torque and radial force are proportional to square of current when the phase current is less than 2A. But if the phase current is greater than 2A, the saturation effect is seen and the torque and radial force are not proportional to the square of current.

In a similar way, by keeping the phase current equal to the constant rated current, the air gap width is varied from 0.4 to 0.8 mm in three steps and the flux density, static torque, and radial force profiles are obtained. The obtained data show decreasing the air gap width increases flux density, the torque is proportional to the inverse of the air gap width and finally, the radial force is proportional to the inverse square of the air gap width and as a result, the acoustic noise power would be related to the fourth power of the inverse of the air gap width.

4. NEW DESIGN OF SRMs

For noise reduction, the air gap width should be increased where radial force is maximized. But if the air gap width increases, the torque value decreases. By investigating the optimization of the torque and radial force profiles, it is deduced that the most influential parameter is the air-gap profile between the stator and the rotor poles. A three-phase 6/4 SRM for which the dimensions are given in Table 1, is used to analyze and compare the results of using the uniform and the non-uniform air-gaps in SRMs. ANSYS, a finite element analysis software, has been used to build and solve a nonlinear magnetic model of the SRM.

Figure 3 shows a design parameter for controlling the air gap profile while the rotating direction of the rotor is considered to be counterclockwise. The design parameter is chosen so that the air-gap becomes narrower as the rotor pole overlaps with the stator pole.
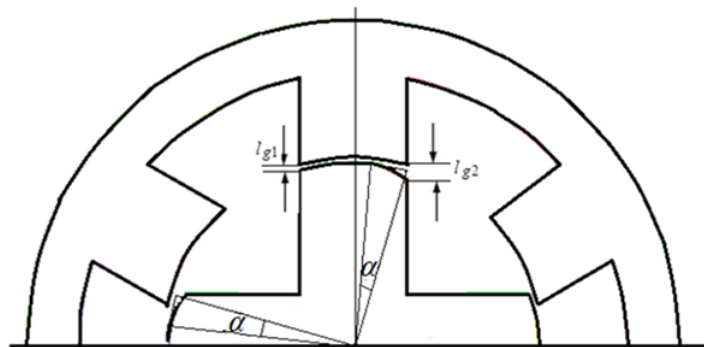

Fig. 3. The designing parameter for the air-gap profile of the SR motor

In Fig. 3, α is the angular interval in which the air-gap width varies between $l_{g1} = 4mm$ and $l_{g2} = 8mm$ while the rotor pole overlaps with the stator pole. The values of α may be between zero and $\theta_r = 42°$.

In order to obtain magnetization characteristic, SRMs are analyzed at the rated current 4A, for six different values of α. Then, dealing with the obtained data, the flux density, torque, and radial force versus the rotor position and the air gap width are plotted in Figs. 4, and 5, respectively.

The profiles of the radial force and torque for different α value versus various rotor angles in a half cycle are shown in Figs. 4 and 5, respectively. These figures show that the radial force and torque are maximized at the same rotor angle while the air gap is uniform (α = 0). For a rotor pole face having a non-uniform air-gap between the rotor and the stator poles (α>0), the maximum of radial force profile is closer to the fully aligned position $(\theta = 45°)$ than the maximum torque profile.
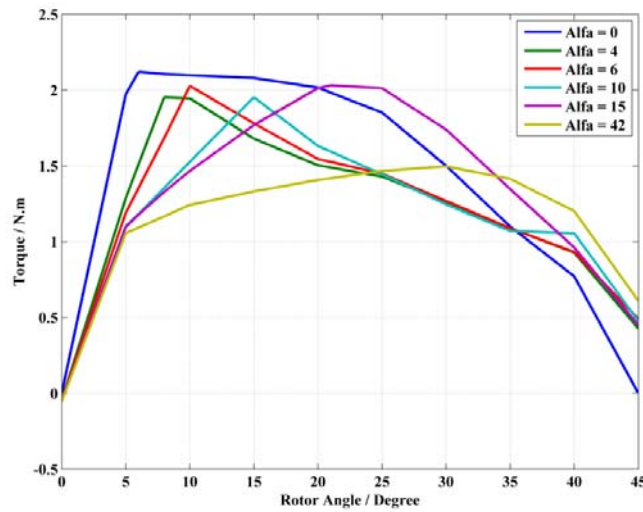

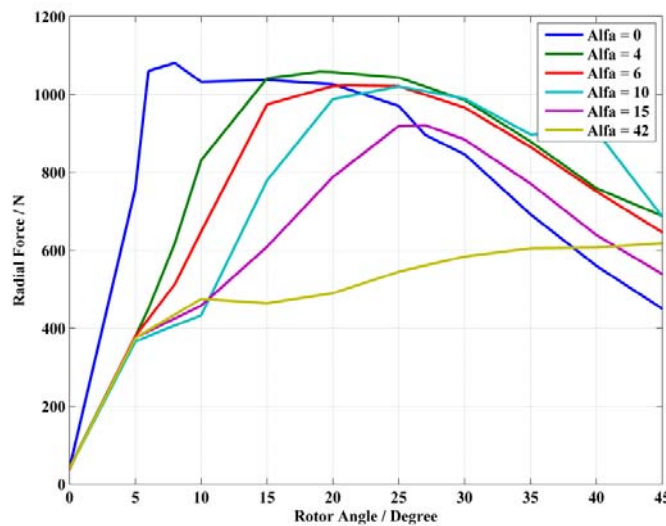Fig. 4. Computed Static Torque profiles for different α values versus various rotor angles

Fig. 5. Computed radial force profiles for different α values versus various rotor angles

For calculating the average air gap width, it has been considered that the shapes of the rotor and the stator in the overlapping area between 0 and α are straight lines. Therefore, the average air gap width in this region is the mean of $l_{g1} = 4mm$ and $l_{g2} = 8mm$. Since the air gap width is equal to $l_{g1} = 4mm$ for angles between α and $42°$, hence the average air gap width in the overlapping area is:

$$lg_{av} = ((42 - \alpha) \times 4 + \alpha \times 6)/42 \qquad (9)$$

From Eqs. (3) and (4), the average torque and the maximum of radial force for the average air gap are calculated and given in Table 2. The average torque is found over that portion of the torque profile that is actually utilized in the motor. Base values in Table 2 are for the case that the air gap between the rotor and stator poles are uniform. The equal torque and radial force are derived as:

$$T_{eq} = T_{base} \frac{lg_{base}}{lg_{av}} \qquad (10)$$

$$F_{req} = F_{rbase} (\frac{lg_{base}}{lg_{av}})^2 \qquad (11)$$

Table 2. The average torque and maximum of radial force for various α values and average air gap

$\alpha/\circ$	0	4	6	10	15	42
lg_{av}	4	4.19	4.29	4.48	4.71	6
$T_{av}(5 < \theta < 35)$	1.86	1.52	1.53	1.48	1.71	1.36
$T_{eq}(5 < \theta < 35)$	1.86	1.77	1.73	1.66	1.57	1.24
F_{rmax1}	1080	1058	1023	1020	921	618
F_{req}	1080	984	941	862	777	480
Torque Ripple	0.55	0.57	0.61	0.60	0.55	0.32

Table 2 shows that: For $\alpha \leq 10$, the average torque decreases and for $\alpha \geq 15$, the average torque increases. For all α, the maximum of radial force increases. Therefore, if we need more torque, then the value of α must be greater than 15 degrees.

In addition, this table shows that in the case of non-uniform air-gap, the torque ripple is high. The phase current changed so that the torque value would be equal to the average torque in all rotor angles. Doing that, the acoustic noise reduces because the torque ripple will be zero. Values of the phase current have been received from the torque profiles.

Figure 6 shows the profile of the phase current for different α values versus various rotor angles. By using these profiles of phase current, torque remains constant and torque ripple will be zero.
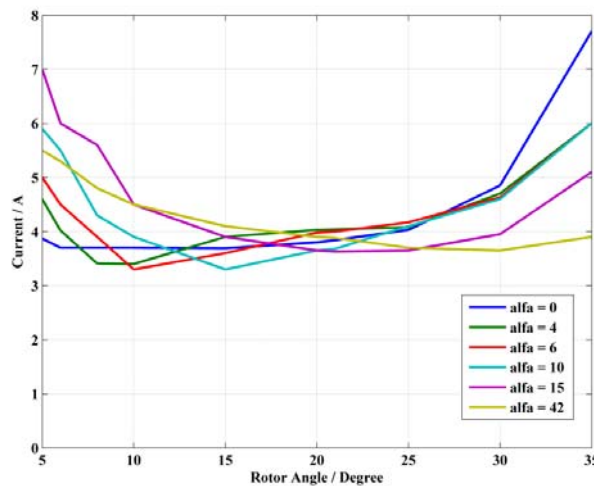

Fig. 6. The phase current for different α values versus various rotor angles

For these values of phase current, the values of the radial force have been obtained from radial force profiles. The average phase currents are calculated for each air gap width and are shown in Table 3. This table shows the average torque and maximum of radial force in static and dynamic cases for various α too.

Table 3. The calculated average phase currents for each air gap width

$\alpha / \circ$	0	4	6	10	15	28
$l_{g_{av}}$	4	4.19	4.29	4.48	4.71	6
i_{av}	4.29	4.22	4.31	4.49	4.70	4.32
T_{avdin}	1.86	1.52	1.53	1.48	1.71	1.36
T_{avsta}	1.86	1.52	1.53	1.48	1.71	1.36
$F_{r_{max din}}$	1019	1071	1048	1068	941	595
$F_{r_{sta}}$	1080	1058	1023	1020	921	618
$\% \Delta F_{r_{max}}$	-5.6%	1.2%	2.4%	4.7%	2.2%	-3.7%
Torque Ripple	0	0	0	0	0	0

Table 3 shows that: The maximum radial force in the dynamic case decreases 5.6% in comparison with the static case in the uniform air gap. In the non-uniform air gap for $\alpha=10^{\circ}$ the maximum radial force in the dynamic case increases 4.7%, but for $\alpha=42^{\circ}$ decreases 3.7%.

In all above cases, the torque ripple is zero.

On the other hand, the acoustic noise power is proportional to the squared amplitude of radial force. Hence, for $\alpha=42^{\circ}$, the acoustic noise power decreases 7.3% and at $\alpha=0^{\circ}$, the acoustic noise power decreases 10.9%.

5. CONCLUSION

In this paper, the effects of the magnetic circuit parameters and phase current on the radial force and the torque ripple of switch reluctance motors have been investigated. Analytical equations demonstrated that the radial force and the torque are proportional to square of the current when the saturation is neglected. Based on these analytical equations, the air gap width is another important factor, because the radial force is inversely proportional to square of the air gap width, and also the torque value is inversely proportional to the air gap width.

Based on the proposed method, by creating the non-uniform air-gap, the radial force decreases. A two-dimensional (2D) finite element (FE) analysis has been carried out on the 6/4 SR motor. To decrease the acoustic noise in the SRM, the air gap width is increased where radial force is maximized. In this method, the radial force decreases while the torque remains constant. By using the method of the compensated current, the ripple torque could be reduced to zero, radial force decreased 3.7%, and the acoustic noise power decreased 7.3% in the non-uniform air gap in comparison with the static case. Furthermore, the radial force decreased 5.6% and the acoustic noise power decreased 10.9% in the uniform air gap in comparison with the static case.

REFERENCES

1. Afjei, E., Hashemipour, O., Nezamabadi, M. M. & Saati, M. A. (2007). A self- tunable sensorless method for rotor position detection in switched reluctance motor drives. *Iranian Journal of Science & Technology, Transaction. B, Engineering*, Vol. 31, No. B3, pp. 317–328.

2. Cameron, D. E., Lang, J. H. & Umans, S. D. (1992). The origin and reduction of acoustic noise in doubly salient variable reluctance motors. *IEEE Trans. on Industry Applic.*, Vol. 28, No. 6, pp. 1250-1255.

3. Ohdachi, Y., Kawase, Y., Miura, Y. & Hayashi, Y. (1997). Optimum design of switched reluctance motors using dynamic finite element analysis. *IEEE Trans. on Magnetics*, Vol. 33, No. 2, pp. 2033–2036.

4. Ozoglu, Y., Garip, M. & Mese, E. (2002). New pole tip shapes mitigating torque ripple in short pitched and fully pitched switched reluctance motors. *Industry Applications Conference*, 37th IAS,1(1), pp. 43–50.

5. Neves, C. G. C., Carlson, R., Sadowski, N., Bastos, J. P. A. & Nau, S. L.(1997). The influence prediction of the current waveforms on the vibrational behavior of switched reluctance motors. *Electric Machines and Drives Conference*, TB1/7.1-TB1/7.3. DOI:10.1109/IEMDC..604211

6. Sahin, F., Ertan, H. B. & Leblebicioglu, K. (2000). Optimum geometry for torque ripple minimization of switched reluctance motors. *IEEE Trans. on Energy Conversion*, Vol. 15, No. 1, pp. 30–39.

7. Sheth, N. K. & Rajagopal, K. R. (2003). Optimum pole arcs for a switched reluctance motor for higher torque with reduced ripple. *IEEE Trans. on Magnetics*, Vol. 39, No. 5, pp. 3214-3216.

8. Sheth, N. K. & Rajagopal, K. R. (2004). Torque profiles of a switched reluctance motor having special pole face shapes and asymmetric stator poles. *IEEE Trans. on Magnetics*, Vol. 40, No. 4, pp. 2035–2037.

9. Lee, J. W., Kim, H. S., Kwon, B. I. & Kim, B. T. (2004) New rotor shape design for minimum torque ripple of SRM using FEM. *IEEE Trans. on Magnetics*, Vol. 40, No. 2, pp. 754–757.

10. Choi, Y. K., Yoon, H. S. & Koh, C. S. (2007). Pole-shape optimization of a switched- reluctance motor for torque ripple reduction. *IEEE Trans. on magnetics*, Vol. 43, No. 4, pp. 1797–1800.

11. Hong, J. P., Ha, K.H. & Lee, J. (2002). Stator pole and yoke design for vibration reduction of switched reluctance motor. *IEEE Trans. on Magnetics*, Vol. 38, No. 2, pp. 929–932.

12. Anwar, M. N. & Husain, I. (2000). Radial force calculation and acoustic noise prediction in switch reluctance machines. *IEEE Trans. on Industry Applic.*, Vol. 36, No. 6, pp. 2242–2249.